

Holographic SIS Josephson Junction

**Yong-Qiang Wang,^a Yu-Xiao Liu,^a Rong-Gen Cai,^b Shingo Takeuchi,^b
Hai-Qing Zhang^b**

^a*Institute of Theoretical Physics, Lanzhou University, Lanzhou 730000, China*

^b*State Key Laboratory of Theoretical Physics, Institute of Theoretical Physics,
Chinese Academy of Sciences, Beijing 100190, China.*

E-mail: yqwang@lzu.edu.cn, liuyx@lzu.edu.cn, cairg@itp.ac.cn,
shingo@itp.ac.cn, hqzhang@itp.ac.cn

ABSTRACT: We construct a holographic model for the superconductor-insulator-superconductor (SIS) Josephson junction at zero temperature by considering a complex scalar field coupled with a Maxwell field in the four-dimensional anti-de Sitter soliton background. From the gravity side we reproduce the sine relation between the Josephson current and the phase difference across the junction. We also study the dependence of the maximal current on the dimension of the condensate operator and on the width of the junction, and obtain expected results.

KEYWORDS: Holography, Josephson junction, AdS Soliton

Contents

1	Introduction	1
2	Setup	3
3	Holographic superconductor/insulator phase transition	5
4	Numerical solutions of the holographic SIS Josephson junction	7
5	Conclusions	9
A	Brief description of Josephson junction	10
B	Analytical study on the superconductor/insulator phase transition	12
B.1	Analytical results of the critical chemical potential for general mass	12
B.2	Analytical relations of $\langle O \rangle \sim (\mu - \mu_c)$ and $\rho \sim (\mu - \mu_c)$	13

1 Introduction

With the help of the AdS/CFT correspondence [1], the superconductivity and superfluid phenomena have been studied intensively on the gravity side in recent years [2–4]. For some reviews, see, for example, [5–7]. One of the interesting phenomena associated with superconductivity is the Josephson effect [8] (a brief description of the Josephson effect is given in appendix A), namely, the effect of electrons tunneling between two superconductors separated by a weak link. The weak link can be a normal conductor or an insulating barrier. Correspondingly the Josephson junction is referred to as the superconductor-normal-superconductor (SNS) or superconductor-insulator-superconductor (SIS) junction, respectively.

Recently, a holographic model for a three-dimensional SNS Josephson junction has been constructed and studied by Horowitz *et al* [9] in an AdS-Schwarzschild black hole background with a Maxwell field and a complex scalar field. The extension to a four-dimensional Josephson junction has been discussed in [10, 11]. The Josephson junction array based on a designer multigravity has been constructed in [12], and the holographic p-wave Josephson junction has also been discussed in [13]. In those works, some familiar features of Josephson junction have been reproduced on the gravity side. Note that in those studies the dual weak link is a normal conductor. Therefore it would be of great interest to construct a holographic model for

a Josephson junction with an insulator link and study its features. This is the aim of the present paper.

In order to build the holographic model for an SIS Josephson junction, we first need a model to realize the superconductor/insulator phase transition. Fortunately such a holographic model was constructed in [14]. There it was shown that in an Einstein-Maxwell-complex scalar field theory with a negative cosmological constant, one can have two phases. One is the AdS soliton solution with a vanishing scalar field. This solution is dual to a confined gauge theory with a mass gap in the AdS boundary, which resembles the insulator phase. The other is the AdS soliton solution with non-vanishing scalar field. When chemical potential increases beyond a certain value μ_c , the above AdS soliton solution turns out to be unstable, a new and stable AdS soliton solution with nontrivial scalar field appears. The new solution is dual to a superconducting phase. In this way one realizes the superconductor/insulator phase transition. The analytical study of the holographic insulator/superconductor phase transition in a five-dimensional AdS soliton spacetime was presented [15]. With the holographic model of superconductor/insulator phase transition, we here construct a holographic model dual to a (1+1)-dimensional SIS Josephson junction in a four-dimensional Einstein-Maxwell-complex scalar theory with a negative cosmological constant.

In the probe limit, by numerically solving the coupled non-linear equations of motion for the Maxwell field and scalar field in an AdS soliton background, we show that the Josephson current is proportional to the sine of the phase difference across the SIS junction. In particular, it is found that the maximum current J_{\max} decreases when the mass square m^2 of the scalar field becomes large or the width L of the junction increases. In addition, the condensation $\langle O \rangle$ dual to the scalar field will also decrease exponentially with respect to L . The coherence length of the junction ξ is found very close to each other from the fittings of the two figures $J_{\max} \sim L$ and $\langle O \rangle \sim L$. We also analytically study this holographic model by virtue of the Sturm-Liouville (S-L) eigenvalue problems [16]. We find that the critical chemical potentials μ_c obtained analytically are in good agreement with the ones from the numerical calculation. Besides, we analytically obtain the critical exponent 1/2 from the relation between the operator condensation and the chemical potential near the critical point, *i.e.*, $\langle O \rangle \propto \sqrt{\mu - \mu_c}$; The charge density ρ is found to be linearly proportional to the chemical potential, *i.e.*, $\rho \propto (\mu - \mu_c)$, which is qualitatively consistent with the numerical calculation.

This paper is organized as follows. In section 2, we set up the gravity dual model of an inhomogeneous superconductor in a four-dimensional Einstein-Maxwell-complex scalar theory with a negative cosmological constant. The holographic insulator/superconductor phase transition is studied in section 3. In section 4, we numerically solve a set of coupled non-linear equations of motion, and study the characteristics of the holographic SIS Josephson junction. Section 5 is devoted to

the conclusions. In appendix A, we briefly describe the Josephson junction, while in appendix B, we give an analytical study on the holographic superconductor/insulator phase transition.

2 Setup

Let us begin with the action of Einstein gravity with a cosmological constant in four dimensions:

$$S = \int d^4x \sqrt{-g} (R - 2\Lambda), \quad (2.1)$$

where the negative cosmological constant Λ is related to ℓ by $\Lambda = -3/\ell^2$, where ℓ is the radius of AdS space. In this system we have a Ricci flat AdS-Schwarzschild black hole solution as

$$ds^2 = -\frac{f(r)}{\ell^2} dt^2 + \ell^2 \frac{dr^2}{f(r)} + r^2(dx^2 + dy^2), \quad (2.2)$$

where $f(r) = r^2 - r_0^3/r$ and $r = r_0$ is the black hole horizon. With the double Wick rotation, we can obtain the so-called AdS soliton solution of this system [17]

$$ds^2 = -r^2 dt^2 + \ell^2 \left(r^2 - \frac{r_0^3}{r} \right)^{-1} dr^2 + r^2 dx^2 + \left(r^2 - \frac{r_0^3}{r} \right) d\chi^2. \quad (2.3)$$

Here the coordinate χ should have a period with $\beta = 4\pi\ell/3r_0$, otherwise there will be a conical singularity at $r = r_0$. In that case $r = r_0$ in the metric (2.3) becomes a tip of a cigar-like geometry. The temperature associated with this AdS soliton vanishes. In addition, let us stress here that the coordinate x is infinitely extended, namely $x \in (-\infty, \infty)$.

Next we consider the matter sector of the model: a Maxwell field coupled with a charged complex scalar field. Its action can be written as

$$S = \int d^4x \sqrt{-g} \left(-\frac{1}{4} F^{\mu\nu} F_{\mu\nu} - |\nabla\psi - iA\psi|^2 - m^2|\psi|^2 \right), \quad (2.4)$$

where $F_{\mu\nu} = \partial_\mu A_\nu - \partial_\nu A_\mu$ is the Maxwell field strength and m is the mass of the scalar field. The equations of motion (EoMs) of the scalar and Maxwell fields read

$$(\nabla_a - iA_a)(\nabla^a - iA^a)\psi - m^2\psi = 0, \quad (2.5)$$

$$\nabla_a F^{ab} - i[\psi^*(\nabla^b - iA^b)\psi - \psi(\nabla^b + iA^b)\psi^*] = 0. \quad (2.6)$$

In order to solve the above equations, we choose an ansatz as

$$\psi = |\psi| e^{i\varphi}, \quad A = (A_t, A_r, A_x, 0), \quad (2.7)$$

where $|\psi|$, φ , A_t , A_r , and A_x are all real functions of coordinates r and x . Instead of A , we work with the gauge-invariant fields: $M = A - d\varphi$.

We are going to study the holographic model in the probe limit. That is, we can ignore the back reaction of the matter fields on the AdS soliton geometry (2.3). In that case, the EoMs for the matter fields in the AdS soliton background become

$$\partial_r^2 |\psi| + \frac{1}{r^2 f} \partial_x^2 |\psi| + \left(\frac{f'}{f} + \frac{2}{r} \right) \partial_r |\psi| + \frac{1}{f} \left(\frac{M_t^2}{r^2} - f M_r^2 - \frac{M_x^2}{r^2} - m^2 \right) |\psi| = 0, \quad (2.8)$$

$$\partial_r M_r + \frac{1}{r^2 f} \partial_x M_x + \frac{2}{|\psi|} \left(M_r \partial_r |\psi| + \frac{M_x}{r^2 f} \partial_x |\psi| \right) + \left(\frac{f'}{f} + \frac{2}{r} \right) M_r = 0, \quad (2.9)$$

$$\partial_r^2 M_t + \frac{1}{r^2 f} \partial_x^2 M_t + \frac{f'}{f} \partial_r M_t - \frac{2|\psi|^2}{f} M_t = 0, \quad (2.10)$$

$$\partial_x^2 M_r - \partial_r \partial_x M_x - 2r^2 |\psi|^2 M_r = 0, \quad (2.11)$$

$$\partial_r^2 M_x - \partial_r \partial_x M_r + \frac{f'}{f} (\partial_r M_x - \partial_x M_r) - \frac{2|\psi|^2}{f} M_x = 0, \quad (2.12)$$

where the superscript a prime denotes the derivative with respect to r . In the following, we will work with the case $m^2 \geq -9/4$, which is above the Breitenlöhner-Freedman bound [18]. Here we have set $\ell = 1$.

Because Eqs. (2.8)-(2.12) are a set of non-linear coupled equations, one cannot solve these equations analytically. However, it is straightforward to solve them numerically. In order to numerically solve Eqs. (2.8)-(2.12), we need to specify the associated boundary conditions in the x and r directions. By imposing the Neumann-like boundary condition suggested in [14], we obtain the asymptotic behaviors of ψ , M_t , M_r and M_x near the tip $r = r_0$ as

$$|\psi| \rightarrow a_0(x) + a_1(x)(r - r_0) + \mathcal{O}((r - r_0)^2), \quad (2.13)$$

$$M_t \rightarrow b_0(x) + b_1(x)(r - r_0) + \mathcal{O}((r - r_0)^2), \quad (2.14)$$

$$M_r \rightarrow c_0(x) + c_1(x)(r - r_0) + \mathcal{O}((r - r_0)^2), \quad (2.15)$$

$$M_x \rightarrow d_0(x) + d_1(x)(r - r_0) + \mathcal{O}((r - r_0)^2). \quad (2.16)$$

Analyzing the EoMs of the scalar field and Maxwell field on the AdS boundary at $r = \infty$, we can take the asymptotic forms as

$$|\psi| \rightarrow \frac{\psi^{(1)}(x)}{r^{(3-\sqrt{9+4m^2})/2}} + \frac{\psi^{(2)}(x)}{r^{(3+\sqrt{9+4m^2})/2}} + \mathcal{O}\left(\frac{1}{r^{(3+\sqrt{9+4m^2})/2+1}}\right), \quad (2.17)$$

$$M_t \rightarrow \mu(x) - \frac{\rho(x)}{r} + \mathcal{O}\left(\frac{1}{r^2}\right), \quad (2.18)$$

$$M_r \rightarrow \mathcal{O}\left(\frac{1}{r^3}\right), \quad (2.19)$$

$$M_x \rightarrow \nu(x) + \frac{J}{r} + \mathcal{O}\left(\frac{1}{r^2}\right), \quad (2.20)$$

where $\psi^{(i)}$ ($i = 1, 2$) are the condensation values of the dual scalar operators $\langle \mathcal{O}_i \rangle$, according to the AdS/CFT dictionary. We can set one of $\psi^{(i)}$ to be vanished. Here

we choose $\psi^{(1)} = 0$. In addition, here μ , ρ , ν and J correspond to the chemical potential, charge density, superfluid velocity and current in the boundary field theory, respectively [19–24].

According to [14], in the above setup we can construct a holographic SIS Josephson junction by adjusting the boundary chemical potential $\mu(x)$: in a region around $x = 0$ along the direction x , $\mu(x)$ is below the critical chemical potential μ_c so that this region behaves like an insulator; while beyond this region $\mu(x)$ is above the critical chemical potential so that those two regions outside the insulator region behave like two superconductors. In this way we construct a holographic SIS Josephson junction. Thus, the gauge invariant phase difference γ across the insulator region can be defined as [9]

$$\gamma = - \int_{-\infty}^{\infty} dx [\nu(x) - \nu(\pm\infty)] . \quad (2.21)$$

The Josephson current J across the Josephson junction has a sine relation to the phase difference γ . We will numerically confirm this in Sec. 4.

3 Holographic superconductor/insulator phase transition

In this section, we will first analyze the critical chemical potential μ_c for the superconductor/insulator phase transition near $x \rightarrow \infty$, in order to give a proper configuration of the chemical potential for the SIS Josephson junction in the next section. In the limit $x \rightarrow \infty$, we assume that all the fields are independent of x , *i.e.*, all the fields are homogeneous in the x -direction. Therefore, Eqs. (2.8)-(2.12) can be reduced to two coupled ordinary differential equations for $|\psi|$ and ϕ as

$$\partial_r^2 |\psi| + \left(\frac{f'}{f} + \frac{2}{r} \right) \partial_r |\psi| + \frac{1}{f} \left(\frac{M_t^2}{r^2} - m^2 \right) |\psi| = 0 , \quad (3.1)$$

$$\partial_r^2 M_t + \frac{f'}{f} \partial_r M_t - \frac{2|\psi|^2}{f} M_t = 0 . \quad (3.2)$$

Here we will numerically solve the EoMs (3.1) and (3.2), while some analytical results will be presented in appendix B, for comparison. We will see that the critical chemical potentials obtained from the two approaches are very close to each other.

The asymptotic forms of $|\psi|$ and M_t near the boundary $r = \infty$ are

$$|\psi| = \frac{\psi^{(1)}}{r^{(3-\sqrt{9+4m^2})/2}} + \frac{\psi^{(2)}}{r^{(3+\sqrt{9+4m^2})/2}} , \quad (3.3)$$

$$M_t = \mu - \frac{\rho}{r} , \quad (3.4)$$

in which the four parameters $(\psi^{(1)}, \psi^{(2)}, \mu, \rho)$ are constants independent of x , μ and ρ are the chemical potential and charge density, respectively, while $\psi^{(1)}$ and $\psi^{(2)}$ are the condensations of dual operators in the superconducting phase.

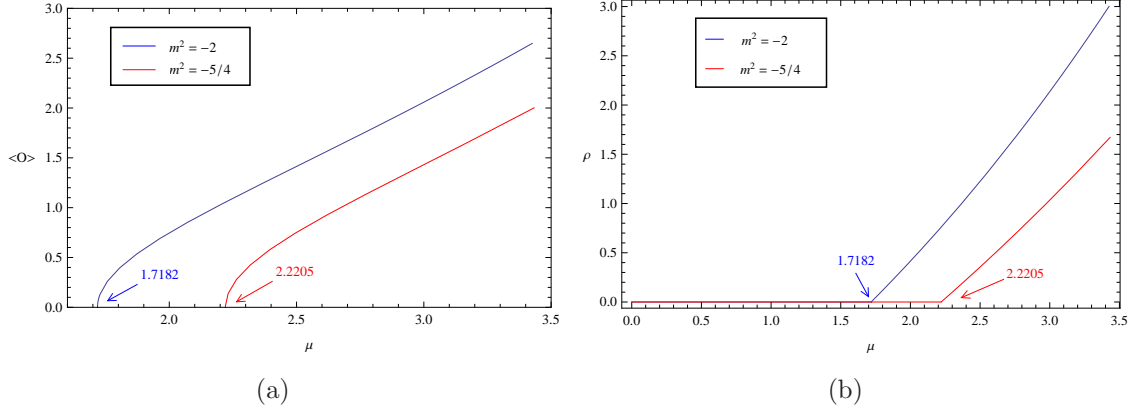


Figure 1. (a) The condensation of the operator $\langle \mathcal{O} \rangle$ versus the chemical potential μ ; (b) The charge density ρ versus the chemical potential μ .

In the numerical calculations, it is convenient to use the shooting method to solve the boundary value problem for the ordinary differential equations (3.1) and (3.2). In the following we will set $r_0 = 1$ and $\ell = 1$. In Fig. 1 we plot the condensation of the operator $\langle \mathcal{O} \rangle$ and charge density ρ as functions of the chemical potential μ . We can see that the charged scalar operator condensates when the chemical potential is above critical value μ_c :

$$\mu_c \approx 1.7182 \quad \text{for } m^2 = -2, \quad (3.5)$$

$$\mu_c \approx 2.2205 \quad \text{for } m^2 = -5/4. \quad (3.6)$$

We can see that the critical chemical potential μ_c grows when m^2 increases, which means that the condensation becomes hard when m^2 increases. In the case of $\mu < \mu_c$, the condensation does not happen and the charge density ρ is always vanishing, one realizes a holographic insulator phase; while $\mu > \mu_c$, the charged operator condensates, which breaks the U(1) gauge symmetry spontaneously. Therefore, when the chemical potential crosses the critical value μ_c , one can realize a holographic insulator/superconductor phase transition. In appendix B, we get analytically the values of the critical chemical potential by using the S-L eigenvalue procedure, which are very close to the ones from the numerical calculations.

In addition, near the critical point, we can read off the critical behavior of the condensation $\langle \mathcal{O} \rangle$ and the charge density ρ from Fig. 1 as

$$\langle \mathcal{O} \rangle \approx 1.3134\sqrt{\mu - \mu_c}, \quad \rho \approx 1.4229(\mu - \mu_c) \quad \text{for } m^2 = -2, \quad (3.7)$$

$$\langle \mathcal{O} \rangle \approx 1.4231\sqrt{\mu - \mu_c}, \quad \rho \approx 1.2758(\mu - \mu_c) \quad \text{for } m^2 = -5/4. \quad (3.8)$$

We can see that $\langle \mathcal{O} \rangle$ is proportional to the square root of $\mu - \mu_c$, and ρ is linearly proportional to $\mu - \mu_c$. We also obtain these square root and linear relations in the analytical study of the critical behavior in appendix B.

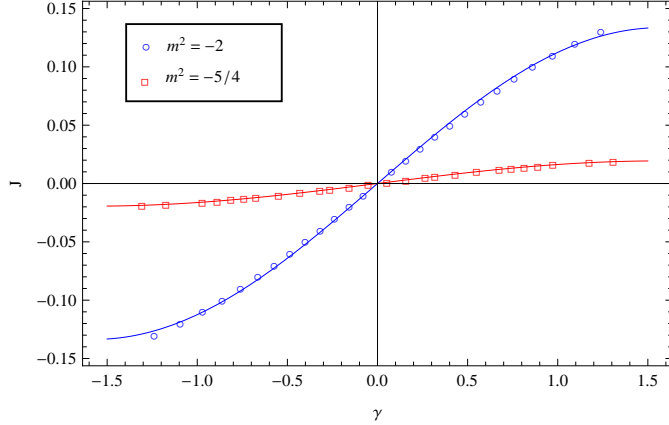


Figure 2. The sine relation between the Josephson current J and the phase difference γ for two different m^2 . Here the parameters are set to $\mu_\infty = 4$, $L = 3$, $\epsilon = 0.4$, $\sigma = 0.5$.

4 Numerical solutions of the holographic SIS Josephson junction

In this section, we will numerically study the holographic SIS Josephson junction. For this aim, following [9], we choose the profile of the chemical potential $\mu(x)$ as

$$\mu(x) = \mu_\infty \left\{ 1 - \frac{1 - \epsilon}{2 \tanh(\frac{L}{2\sigma})} \left[\tanh\left(\frac{x + \frac{L}{2}}{\sigma}\right) - \tanh\left(\frac{x - \frac{L}{2}}{\sigma}\right) \right] \right\}, \quad (4.1)$$

where $\mu_\infty \equiv \mu(\infty) = \mu(-\infty)$ is the value of the chemical potential μ at $x = \pm\infty$, and the parameters L , σ and ϵ are the width, steepness and depth of the junction, respectively. Actually, we can suitably choose the parameters in $\mu(x)$ so that

$$\begin{cases} \mu(x) < \mu_c, & \text{for } -L/2 < x < L/2, \\ \mu(x) > \mu_c, & \text{for } x < -L/2 \text{ and } x > L/2. \end{cases} \quad (4.2)$$

Thus the central part of the junction is a holographic insulator while the two sides are two holographic superconductors. Such a junction is an SIS Josephson junction as we expected.

With the above chemical potential, we can numerically solve the set of coupled equations (2.8)-(2.12) by virtue of the spectral method. In Fig. 2, we plot the current J as a function of the phase difference γ with $\mu_\infty = 4$, $L = 3$, $\epsilon = 0.4$, $\sigma = 0.5$. The circles and the squares are from the numerical calculations while the solid lines are the fittings of them. The relation between J and γ can be fitted as

$$J \approx 0.1336 \sin \gamma, \quad \text{for } m^2 = -2, \quad (4.3)$$

$$J \approx 0.0194 \sin \gamma, \quad \text{for } m^2 = -5/4. \quad (4.4)$$

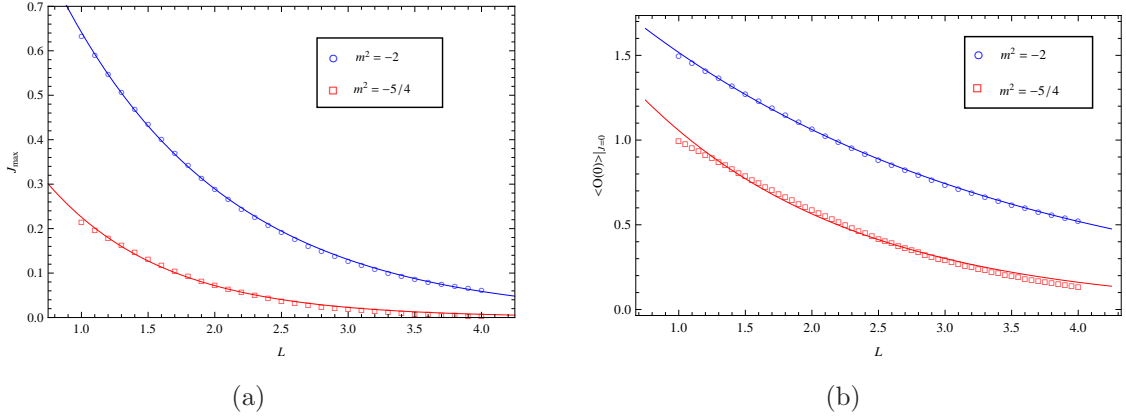


Figure 3. (a) The maximal current J_{\max} versus the width L of the junction; (b) The condensation $\langle \mathcal{O}(0) \rangle_{J=0}$ versus the width L of the junction, for two different m^2 . Here the parameters are chosen as $\mu_\infty = 4$, $\epsilon = 0.4$, and $\sigma = 0.5$.

We see that the Josephson current J is indeed proportional to the sine of the phase difference γ , which realizes the SIS Josephson junction. Further we find that the amplitude of the sine relation or the maximum current J_{\max} decrease when m^2 becomes large. The relation between the maximum current J_{\max} and the width of the junction L is plotted in Fig. 3(a); And the relation between the condensation $\langle \mathcal{O}(0) \rangle = \psi^{(2)}$ at zero current and L is given in Fig. 3(b). The circles and squares are obtained from the numerical calculations while the solid lines are the fittings of them. From appendix A, one learns that the dependencies of J_{\max} and $\langle \mathcal{O}(0) \rangle_{J=0}$ on L behave like

$$J_{\max} = A_0 e^{-\frac{L}{\xi}}, \quad (4.5)$$

$$\langle \mathcal{O}(0) \rangle_{J=0} = A_1 e^{-\frac{L}{2\xi}}, \quad (4.6)$$

where ξ is the coherence length of the SIS Josephson junction, while A_0 and A_1 are two constants. In our holographic model, the fitted result in Fig. 3(a) gives

$$J_{\max} \approx 1.4230 e^{-L/1.2552}, \quad \text{for } m^2 = -2, \quad (4.7)$$

$$J_{\max} \approx 0.7107 e^{-L/0.8720}, \quad \text{for } m^2 = -5/4, \quad (4.8)$$

while in Fig. 3(b) the fitted result has the forms

$$\langle \mathcal{O} \rangle \approx 2.1671 e^{-L/(2 \times 1.4015)}, \quad \text{for } m^2 = -2, \quad (4.9)$$

$$\langle \mathcal{O} \rangle \approx 1.9783 e^{-L/(2 \times 0.7969)}, \quad \text{for } m^2 = -5/4. \quad (4.10)$$

The coherence lengths ξ fitted from the two plots are consistent to each other within 10.5% error. Thus we see that in the holographic model, the familiar results (4.5) and (4.6) for the SIS Josephson junction can be indeed reproduced on the gravity side.

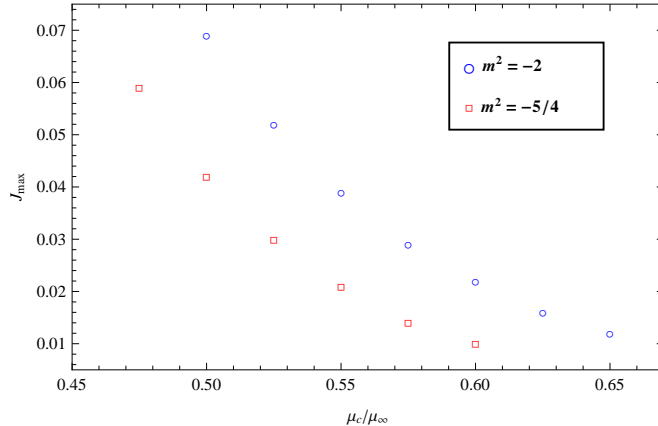


Figure 4. The maximum current J_{\max} versus μ_c/μ_∞ for two different m^2 . The parameters are set to $L = 3$, $\epsilon = 0.4$, $\sigma = 0.5$.

We also plot the relation between the maximum current J_{\max} and μ_c/μ_∞ in Fig. 4, from which one can see that J_{\max} will decrease when μ_c/μ_∞ increases, and as μ_c/μ_∞ goes close to 1, the current is suppressed very much. This result is expected, because when $\mu_c/\mu_\infty \rightarrow 1$, the chemical potential in both sides of the insulator just reaches the critical value. In this case the superconducting current is very small and the “strength” of their superconductivity is rather weak. We expect that the current vanishes finally at $\mu_c/\mu_\infty = 1$. On the other hand, we can see the maximal current quickly increases when μ_c/μ_∞ becomes small. This tendency is also understandable, since in this case the two sides of the junction are in the superconducting phases far from the critical point, and the “strength” of the superconductivity becomes very strong.

5 Conclusions

In this paper, we studied the holographic insulator/superconductor phase transition in a four-dimensional AdS soliton background. It was found that the critical chemical potential μ_c increases when the mass square m^2 of the scalar field grows. We investigated the behaviors of the condensation $\langle \mathcal{O} \rangle$ and the charge density ρ , and found that the numerical results near the critical point are in good agreement with those obtained from an analytical procedure.

Furthermore, with the help of the holographic superconductor/insulator model, suitably setting the profile of the chemical potential $\mu(x)$ on the AdS boundary, and following [9], we constructed a holographic model for an SIS Josephson junction. We numerically solved a set of non-linear equations of motion and confirmed that the Josephson current J of the SIS junction is indeed proportional to the sine of the phase difference γ across the junction. Besides, we also shown that the maximum

current J_{\max} decreases when the mass square of the scalar field becomes large. We further studied the dependence of J_{\max} and $\langle \mathcal{O}(0) \rangle|_{J=0}$ on the width L of the junction, and found that J_{\max} and $\langle \mathcal{O}(0) \rangle|_{J=0}$ are suppressed exponentially when L increases. Thus we reproduced these main features of Josephson junction on the gravity side. In addition, J_{\max} was found to be a decreasing function of μ_c/μ .

The Josephson effect is an important phenomenon associated with superconductor. Some features of Josephson junction are robust such as the sine relation between the current and the phase difference across the junction. For the holographic models of the SNS Josephson junction constructed in [9] and the SIS Josephson junction discussed in this paper, one can indeed confirm this relation on the gravity side. Therefore, it is interesting to further study the holographic model for the superconductor-superconductor-superconductor junction, where the middle superconductor is different from the other two superconductors. We expect that the sine relation will also hold in that case. Finally let us mention here that it is also of great interest to investigate the effect of magnetic field on the Josephson junction from the holographic point of view [33].

Acknowledgments

S.T and H.Q.Z would like to thank the hospitalities of Lanzhou University. Y.Q.W and Y.X.L were supported in part by the National Natural Science Foundation of China (No. 11005054 and No. 11075065), and in part by the Fundamental Research Funds for the Central Universities (No. lzujbky-2012-18 and No. lzujbky-2012-k30). R.G.C and H.Q.Z were supported in part by the National Natural Science Foundation of China (No.10821504, No.10975168 and No.11035008), and in part by the Ministry of Science and Technology of China under Grant No. 2010CB833004.

A Brief description of Josephson junction

To be complete, we will briefly review the Josephson junction in this appendix. Considering two superconductors separated by an insulating barrier, in 1962, Josephson [8] made a remarkable prediction that there exists a current flowing across the middle insulator even when there is no voltage difference between these two superconductors. This supercurrent is caused by quantum tunneling of Cooper pair. This is just the Josephson effect. The current is related to the difference of phases of macroscopic wave functions in the two superconductors:

$$J = J_{\max} \sin \gamma, \tag{A.1}$$

where J_{\max} is the maximal current (critical current) and γ is the phase difference of the macroscopic wave function $\psi = |\psi|e^{i\theta}$ in two superconductors, which is in-

roduced as an order parameter in the Ginzburg-Landau model. This remarkable prediction was experimentally confirmed soon [25].

The Josephson's prediction was based on a microscopic theoretical analysis of quantum mechanical tunneling of electrons through the insulating barrier layer. But in fact, this Josephson effect is much more general, it occurs when two superconductors are connected by a weak link, the latter is called Josephson junction. The weak link can be an insulator as Josephson originally proposed, or a normal metal layer, or simply a short and narrow constriction. In those cases, the Josephson junction are called SIS, SNS and SCS junctions, respectively.

Suppose that $\psi_1 = |\psi_1|e^{i\theta_1}$ and $\psi_2 = |\psi_2|e^{i\theta_2}$ are two macroscopic wave functions describing these two superconductors. Due to the weak coupling between them, the two wave functions are not independent of each other. Instead they relate to each other as: $\partial_x\psi_1 = K\psi_2$ and $\partial_x\psi_2 = -K\psi_1$, where K is a parameter representing the strength of the weak coupling, and x is the direction perpendicular to the boundary surface between superconductor and insulator. In the case with two identical superconductors, one has $|\psi_1| = |\psi_2| \equiv |\psi| = \sqrt{\rho_0}$, where ρ_0 is the density of Cooper pair. Generally speaking, the supercurrent associated with a macroscopic wave function $\Psi(\mathbf{r})$ is given as $\mathbf{J} = -i\frac{e^*\hbar}{2m^*}(\Psi^*\nabla\Psi - \Psi\nabla\Psi^*)$, where e^* and m^* mean the charge and the mass of the Cooper pair. From this, one can obtain the Josephson current flowing over the weak link by substituting $\psi_1 = |\psi|e^{i\theta_1}$ and $\psi_2 = |\psi|e^{i\theta_2}$ into the supercurrent equation as

$$J_x = J_{\max} \sin(\theta_2 - \theta_1) = J_{\max} \sin \gamma, \quad (\text{A.2})$$

along the direction x , where $J_{\max} \equiv K\frac{e^*\hbar}{m^*}\rho_0$ is the maximal Josephson current.

The maximal Josephson current J_{\max} is closely related to the width L of the weak link (see, for example, [26]) as

$$J_{\max} \sim \rho_0 e^{-L/\xi}, \quad (\text{A.3})$$

where the coherence length ξ , which is one of the characteristic scales of superconductors, can vary with superconducting materials. The maximal current is also proportional to the density of Cooper pair in the weak link as $J_{\max} \sim |\psi|^2$. Considering the relation between the number density ρ and the condensation $\langle\mathcal{O}\rangle$: $\rho \sim \langle\mathcal{O}\rangle^2$, see, for example, (B.19), one has

$$\langle\mathcal{O}\rangle \sim J_{\max}^{1/2} \sim e^{-L/2\xi}, \quad (\text{A.4})$$

in the weak link of the Josephson junction. Indeed, in our holographic model of SIS Josephson junction, we have reproduced the three relations (A.1), (A.3) and (A.4).

B Analytical study on the superconductor/insulator phase transition

In this appendix we will take advantage of the S-L method [16] to analytically study the homogenous solutions of the equations of motion near the critical point of the phase transition. For further applications of the S-L method to other holographic superconductor models, see Refs. [15, 27–32].

B.1 Analytical results of the critical chemical potential for general mass

In this case all matter fields are independent of the coordinate x . By setting $z = 1/r$, the EoMs (2.8) and (2.10) are reduced to (we have set $M_t = \phi$ here)

$$\partial_z^2 \psi(z) - \frac{2+z^3}{z-z^4} \partial_z \psi(z) + \frac{\phi(z)^2 z^2 - m^2}{z^2(1-z^3)} \psi(z) = 0, \quad (\text{B.1})$$

$$\partial_z^2 \phi(z) - \frac{3z^2}{1-z^3} \partial_z \phi(z) - \frac{2\psi(z)^2}{z^2(1-z^3)} \phi(z) = 0. \quad (\text{B.2})$$

At the critical point, the scalar field ψ vanishes. Near the critical point, we can introduce a trial function $F(z)$ into the asymptotical form of ψ near the boundary like

$$\psi|_{z \rightarrow 0} \sim \langle O \rangle z^\Delta F(z), \quad (\text{B.3})$$

where $\Delta \equiv 3/2 + \sqrt{9/4 + m^2}$ is the conformal dimension of the dual operator. It is easy to see from the boundary conditions of ψ that $F(0) = 1$. For simplicity, we can set $F'(0) = 0$. Therefore, the simplest form of $F(z)$ is $F(z) = 1 - \alpha z^2$, where α is a constant. Besides, near the critical point of the phase transition, $\phi(z) \sim \mu$. Thus, substituting formula (B.3) into Eq. (B.1), and multiplying $K(z) \equiv z^{-2(1-\Delta)}(-1+z^3)$ to both sides, we can reach

$$\partial_z \left(K(z) \partial_z F(z) \right) + \left(-P(z) + Q(z) \mu^2 \right) F(z) = 0, \quad (\text{B.4})$$

with

$$P(z) \equiv -z^{-2(2-\Delta)} [m^2 + \Delta \{3 - \Delta(1 - z^3)\}] \quad \text{and} \quad Q(z) \equiv -z^{-2(1-\Delta)}. \quad (\text{B.5})$$

Through the S-L eigenvalue method, we can obtain the critical chemical potential by minimizing the following functional at some value of α ,

$$\mu^2 = \frac{\int_0^1 dz \{ K(z) (\partial_z F(z))^2 + P(z) F(z)^2 \}}{\int_0^1 dz Q(z) F^2(z)}. \quad (\text{B.6})$$

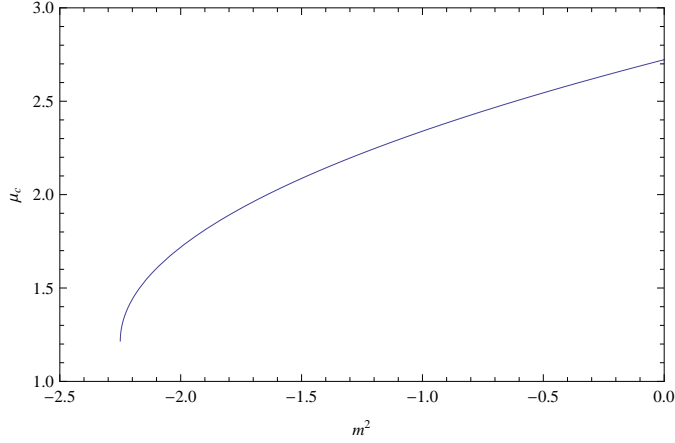


Figure 5. The critical chemical potential μ_c as a function of the mass square m^2 . The plot is obtained from minimizing the formula (B.6) for certain α .

Fig.5 plots the relation between μ_c and m^2 . In particular, the critical chemical potentials for the cases of $m^2 = -2$ and $-5/4$ are, respectively,

$$\mu_c \approx 1.71884 \quad \text{for} \quad m^2 = -2, \quad (\text{B.7})$$

$$\mu_c \approx 2.22116 \quad \text{for} \quad m^2 = -5/4. \quad (\text{B.8})$$

We see that these values (B.7) and (B.8) of the critical chemical potential are in good agreement with the numerical results (3.5) and (3.6), respectively.

B.2 Analytical relations of $\langle O \rangle \sim (\mu - \mu_c)$ and $\rho \sim (\mu - \mu_c)$

Near the critical point $\mu \rightarrow \mu_c$, the condensation value of the operator $\langle O \rangle$ is very small, therefore, we can expand $\phi(z)$ in the series of $\langle O \rangle$ like

$$\phi \sim \mu_c + \langle O \rangle \zeta(z), \quad (\text{B.9})$$

where, $\zeta(z)$ is a coefficient function independent of $\langle O \rangle$. We can easily find that the behavior of $\phi(z)$ near the tip of the background geometry imposes

$$\zeta(1) = 0. \quad (\text{B.10})$$

The EoMs of ζ can be obtained from Eqs. (B.2), (B.3) and (B.9) by taking the leading order of $\langle O \rangle$ as

$$\partial_z^2 \zeta(z) - \frac{3z^2}{1-z^3} \partial_z \zeta(z) = \frac{2\mu_c \langle O \rangle z^{2\Delta-2} F(z)^2}{1-z^3}. \quad (\text{B.11})$$

Multiplying $T(z) = -1 + z^3$ to both sides of (B.11), we arrive at

$$\frac{d}{dz} \left(T(z) \partial_z \zeta(z) \right) = -2\mu_c \langle O \rangle z^{2\Delta-2} F(z)^2. \quad (\text{B.12})$$

Integrating both sides of the above equation, we can get the Neumann boundary condition of ζ near $z \rightarrow 0$ as

$$\begin{aligned}
(-1 + z^3)\partial_z\zeta(z)|_0^1 &= \partial_z\zeta(z)|_{z \rightarrow 0} \\
&= -2\mu_c\langle O \rangle \int_0^1 dz z^{2\Delta-2} F(z)^2 \\
&= -2\mu_c\langle O \rangle \left(\frac{1}{2\Delta-1} - \frac{2\alpha}{2\Delta+1} + \frac{\alpha^2}{2\Delta+3} \right). \quad (\text{B.13})
\end{aligned}$$

Therefore, from Eq. (B.11) and the boundary conditions (B.10) and (B.13) of ζ , we can obtain

$$\begin{aligned}
\zeta(z) &= \frac{1}{9}\mu_c\langle O \rangle \left\{ -\frac{18\alpha^2 z^{2\Delta+1}}{4\Delta^2 + 8\Delta + 3} - \frac{9z^{2\Delta}}{\Delta - 2\Delta^2} \right. \\
&\quad + \frac{18\alpha^2 z^{2\Delta+1}}{4\Delta^2 + 8\Delta + 3} {}_2F_1\left(1, \frac{1}{3}(2\Delta + 1); \frac{2(\Delta + 2)}{3}; z^3\right) \\
&\quad - \frac{18\alpha z^{2\Delta+2}}{2\Delta^2 + 3\Delta + 1} {}_2F_1\left(1, \frac{2(\Delta + 1)}{3}; \frac{1}{3}(2\Delta + 5); z^3\right) \\
&\quad + \frac{18z^{2\Delta+3}}{4\Delta^2 + 4\Delta - 3} {}_2F_1\left(1, \frac{2\Delta}{3} + 1; \frac{2\Delta}{3} + 2; z^3\right) \\
&\quad + \frac{1}{\Delta(2\Delta - 1)(2\Delta + 1)(2\Delta + 3)} \left[6\alpha^2\Delta(4\Delta^2 - 1)\psi^{(0)}\left(\frac{2\Delta}{3} + \frac{1}{3}\right) \right. \\
&\quad + 2\alpha^2\Delta(2\Delta - 1)\left(\sqrt{3}\pi(2\Delta + 1) + 9\right) - 4\sqrt{3}\pi\alpha\Delta(4\Delta^2 + 4\Delta - 3) \\
&\quad - 12\alpha\Delta(4\Delta^2 + 4\Delta - 3)\psi^{(0)}\left(\frac{2(\Delta + 1)}{3}\right) + (2\sqrt{3}\pi\Delta - 9)(4\Delta^2 + 8\Delta + 3) \\
&\quad + 6\Delta(4\Delta^2 + 8\Delta + 3)\psi^{(0)}\left(\frac{2\Delta}{3} + 1\right) + 3\Delta\left(\alpha^2(4\Delta^2 - 1) + \alpha(-8\Delta^2 - 8\Delta + 6) \right. \\
&\quad \left. + 4\Delta^2 + 8\Delta + 3\right) \left(-\log(z^2 + z + 1) + 2\log(1 - z) - 2\sqrt{3}\tan^{-1}\left(\frac{2z + 1}{\sqrt{3}}\right) \right. \\
&\quad \left. \left. + 2\gamma + \log(27)\right) \right] \left. \right\}, \quad (\text{B.14})
\end{aligned}$$

where, ${}_2F_1(a, b; c, d)$ is the hypergeometric function, $\psi^{(0)}$ is the digamma function and γ is the Euler gamma function.

Near the boundary $z = 0$, we can expand $\phi(z)$ from (2.18) and (B.9) as

$$\phi(z) \sim \mu - \rho z \sim \mu_c + \langle O \rangle \left(\zeta(0) + \zeta'(0)z + \frac{1}{2}\zeta''(0)z^2 + \dots \right). \quad (\text{B.15})$$

Therefore, comparing the coefficients of the z^0 term of (B.15) we have

$$\mu - \mu_c \sim \langle O \rangle \zeta(0) \propto \langle O \rangle^2. \quad (\text{B.16})$$

From the critical values of μ_c and the corresponding α above, we can reach

$$\langle O \rangle \approx 1.08790\sqrt{\mu - \mu_c}, \quad \text{for } m^2 = -2, \quad (\text{B.17})$$

$$\langle O \rangle \approx 1.09588\sqrt{\mu - \mu_c}, \quad \text{for } m^2 = -5/4. \quad (\text{B.18})$$

which are qualitatively consistent with the numerical results in (3.7) and (3.8). The critical exponent 1/2 between the condensation value and the chemical potential is also consistent with the one from the mean field theory. Besides, we notice from the z^1 terms of both sides of (B.15) that

$$\rho \sim -\langle O \rangle \zeta'(0) \propto \langle O \rangle^2 \propto (\mu - \mu_c). \quad (\text{B.19})$$

This linear relation between the charge density and the chemical potential is also qualitatively consistent with the numerical results in (3.7) and (3.8). From (B.19) we obtain

$$\rho \approx 1.05323(\mu - \mu_c), \quad \text{for } m^2 = -2, \quad (\text{B.20})$$

$$\rho \approx 0.95214(\mu - \mu_c), \quad \text{for } m^2 = -5/4. \quad (\text{B.21})$$

Here the discrepancy in the numerical factors from both methods in the relations $\langle O \rangle \sim \sqrt{\mu - \mu_c}$ and $\rho \sim (\mu - \mu_c)$ might be due to the fact that we have only adopted a simplest form of the trial function $F(z)$ in (B.3), if we introduce higher order terms of z into the trial function, this may improve the discrepancy of the numerical factors.

References

- [1] J. M. Maldacena, *The Large N limit of superconformal field theories and supergravity*, Adv. Theor. Math. Phys. **2**, 231 (1998) [Int. J. Theor. Phys. **38**, 1113 (1999)] [arXiv:hep-th/9711200].
- [2] S. S. Gubser, *Breaking an Abelian gauge symmetry near a black hole horizon*, Phys. Rev. **D 78**, 065034 (2008) [arXiv:0801.2977 [hep-th]].
- [3] S. A. Hartnoll, C. P. Herzog and G. T. Horowitz, *Building a Holographic Superconductor*, Phys. Rev. Lett. **101**, 031601 (2008) [arXiv:0803.3295 [hep-th]].
- [4] S. A. Hartnoll, C. P. Herzog and G. T. Horowitz, *Holographic Superconductors*, JHEP **0812**, 015 (2008) [arXiv:0810.1563 [hep-th]].
- [5] S. A. Hartnoll, *Lectures on holographic methods for condensed matter physics*, Class. Quant. Grav. **26**, 224002 (2009) [arXiv:0903.3246 [hep-th]].
- [6] C. P. Herzog, *Lectures on Holographic Superfluidity and Superconductivity*, J. Phys. **A 42**, 343001 (2009) [arXiv:0904.1975 [hep-th]].
- [7] G. T. Horowitz, *Introduction to Holographic Superconductors*, arXiv:1002.1722 [hep-th].

- [8] B. D. Josephson, *Possible new effects in superconductive tunnelling*, Phys. Lett. **1**, 251 (1962).
- [9] G. T. Horowitz, J. E. Santos and B. Way, *A Holographic Josephson Junction*, Phys. Rev. Lett. **106**, 221601 (2011) [arXiv:1101.3326 [hep-th]].
- [10] Y. Q. Wang, Y. X. Liu and Z. H. Zhao, *Holographic Josephson Junction in 3+1 dimensions*, arXiv:1104.4303 [hep-th].
- [11] M. Siani, *On inhomogeneous holographic superconductors*, arXiv:1104.4463 [hep-th].
- [12] E. Kiritsis and V. Niarchos, *Josephson Junctions and AdS/CFT Networks*, JHEP **1107**, 112 (2011) [arXiv:1105.6100 [hep-th]].
- [13] Y. -Q. Wang, Y. -X. Liu and Z. -H. Zhao, *Holographic p-wave Josephson junction*, arXiv:1109.4426 [hep-th].
- [14] T. Nishioka, S. Ryu and T. Takayanagi, *Holographic Superconductor/Insulator Transition at Zero Temperature*, JHEP **1003**, 131 (2010) [arXiv:0911.0962 [hep-th]].
- [15] R. -G. Cai, H. -F. Li and H. -Q. Zhang, *Analytical Studies on Holographic Insulator/Superconductor Phase Transitions*, Phys. Rev. D **83**, 126007 (2011) [arXiv:1103.5568 [hep-th]].
- [16] G. Siopsis and J. Therrien, *Analytic calculation of properties of holographic superconductors*, JHEP **1005**, 013 (2010) [arXiv:1003.4275 [hep-th]].
- [17] G. T. Horowitz and R. C. Myers, *The AdS/CFT correspondence and a new positive energy conjecture for general relativity*, Phys. Rev. D **59**, 026005 (1998) [hep-th/9808079].
- [18] P. Breitenlohner and D. Z. Freedman, *Positive Energy in anti-De Sitter Backgrounds and Gauged Extended Supergravity*, Phys. Lett. **B 115**, 197 (1982).
- [19] P. Basu, A. Mukherjee and H. -H. Shieh, *Supercurrent: Vector Hair for an AdS Black Hole*, Phys. Rev. D **79**, 045010 (2009) [arXiv:0809.4494 [hep-th]].
- [20] C. P. Herzog, P. K. Kovtun and D. T. Son, *Holographic model of superfluidity*, Phys. Rev. D **79**, 066002 (2009) [arXiv:0809.4870 [hep-th]].
- [21] D. Arean, M. Bertolini, J. Evslin and T. Prochazka, *On Holographic Superconductors with DC Current*, JHEP **1007**, 060 (2010) [arXiv:1003.5661 [hep-th]].
- [22] J. Sonner and B. Withers, *A gravity derivation of the Tisza-Landau Model in AdS/CFT*, Phys. Rev. D **82**, 026001 (2010) [arXiv:1004.2707 [hep-th]].
- [23] G. T. Horowitz and M. M. Roberts, *Holographic Superconductors with Various Condensates*, Phys. Rev. D **78**, 126008 (2008) [arXiv:0810.1077 [hep-th]].
- [24] D. Arean, P. Basu and C. Krishnan, *The Many Phases of Holographic Superfluids*, JHEP **1010**, 006 (2010) [arXiv:1006.5165 [hep-th]].
- [25] P. W. Anderson and J. M. Rowell, *Probable Observation of the Josephson Superconducting Tunneling Effect*, Phys. Rev. Lett. **10**, 230 (1963).

- [26] M. Tinkham, *Introduction to Superconductivity (Second Edition), 1996, Mac-Graw-Hill, Inc.*
- [27] H. -B. Zeng, X. Gao, Y. Jiang and H. -S. Zong, *Analytical Computation of Critical Exponents in Several Holographic Superconductors*, JHEP **1105**, 002 (2011) [arXiv:1012.5564 [hep-th]].
- [28] H. -F. Li, R. -G. Cai and H. -Q. Zhang, *Analytical Studies on Holographic Superconductors in Gauss-Bonnet Gravity*, JHEP **1104**, 028 (2011) [arXiv:1103.2833 [hep-th]].
- [29] Q. Pan, J. Jing and B. Wang, *Analytical investigation of the phase transition between holographic insulator and superconductor in Gauss-Bonnet gravity*, JHEP **1111**, 088 (2011) [arXiv:1105.6153 [gr-qc]].
- [30] D. Momeni, E. Nakano, M. R. Setare and W. -Y. Wen, *Analytical study of critical magnetic field in a holographic superconductor*, arXiv:1108.4340 [hep-th].
- [31] R. -G. Cai, L. Li, H. -Q. Zhang and Y. -L. Zhang, *Magnetic Field Effect on the Phase Transition in AdS Soliton Spacetime*, Phys. Rev. D **84**, 126008 (2011) [arXiv:1109.5885 [hep-th]].
- [32] C. O. Lee, *The holographic superconductors in higher-dimensional AdS soliton*, to appear in European Physical Journal C, arXiv:1202.5146 [gr-qc].
- [33] J. M. Rowell, *Magnetic Field Dependence of the Josephson Tunnel Current*, Phys. Rev. Lett. **11**, 200 (1963).